Quantum simulations of hydrodynamics via the Madelung transformation

Quantum simulations of hydrodynamics via the Madelung transformation

Julien Zylberman,[1] Giuseppe Di Molfetta,[2] Marc Brachet,[3] Nuno F. Loureiro,[4] and Fabrice Debbasch[1]
[1]*Sorbonne Université, Observatoire de Paris, Université PSL, CNRS, LERMA, F-75005 Paris, France*
[2]*CNRS, LIS, Aix-Marseille Université, Université de Toulon, Marseille, France*
[3]*Laboratoire de Physique de l'École Normale Supérieure, ENS, Université PSL, CNRS, Sorbonne Université, Université de Paris, F-75005 Paris, France*
[4]*Plasma Science and Fusion Center, Massachusetts Institute of Technology, Cambridge, Massachusetts 02139, USA*

(Received 21 February 2022; accepted 6 July 2022; published 7 September 2022)

Developing numerical methods to simulate efficiently nonlinear fluid dynamics on universal quantum computers is a challenging problem. In this paper, a generalization of the Madelung transform is defined to solve quantum relativistic charged fluid equations interacting with external electromagnetic forces via the Dirac equation. The Dirac equation is discretized into discrete-time quantum walks which can be efficiently implemented on universal quantum computers. A variant of this algorithm is proposed to implement simulations using current noisy intermediate scale quantum (NISQ) devices in the case of homogeneous external forces. High resolution (up to $N = 2^{17}$ grid points) numerical simulations of relativistic and nonrelativistic hydrodynamical shocks on current IBM NISQs are performed with this algorithm. This paper demonstrates that fluid dynamics can be simulated on NISQs, and opens the door to simulating other fluids, including plasmas, with more general quantum walks and quantum automata.

DOI: 10.1103/PhysRevA.106.032408

I. INTRODUCTION

The so-called second quantum revolution is possibly one of the greatest scientific and technological challenges of the 21st century. One of the cornerstones of that revolution is quantum computing, i.e., the possibility of using quantum properties of matter to outperform current classical computers, at least for several standard computations. Quantum simulation originated with Feynman [1], who suggested using quantum systems to simulate efficiently other, more complex, quantum, and possibly also classical, systems.

Efficiently simulating the dynamics of both classical and quantum fluids, be they relativistic or not, is a long-standing problem in applied mathematics and the applications in engineering and fundamental science cannot be overestimated. For example, nonquantum nonrelativistic hydrodynamics is necessary in studying pipe flows and porous materials (including the earth, with applications in, e.g., oil prospecting), as well as aerodynamics (with applications in the transport industry). Traditional quantum hydrodynamics is necessary to describe superfluids and Bose condensates [2–4]. Relativistic (nonquantum) magnetohydrodynamics is useful to the study of plasmas, both earth- and space-bound—for example, to describe accretion around a black hole [5]. Finally, relativistic quantum magnetohydrodynamics is useful in all situations where extreme plasmas come into play, for example, in astrophysical relativistic compact objects like neutron stars [6].

The difficulty encountered in trying to simulate hydrodynamics on classical computers is perhaps best illustrated by the fundamental classical, nonquantum, and nonrelativistic problem of fully developed incompressible turbulence. In this case, the Reynolds number R is the single relevant dimensionless number and the unknown turbulent statistical laws one is interested in occur in the asymptotic regime $R \to \infty$, see, for example, Ref. [7]. It can be shown (see Chap. 7 of Ref. [7]) that the typical amount of computer memory needed for the classical simulation grows as $O(R^{9/4})$ and that the total computational work needed to integrate the equations for a fixed number of large eddies turnover times grows as $O(R^3)$. These scaling laws clearly illustrate the difficulties encountered when one tries to understand the practical important problem of fully developed turbulence through classical simulations. To have an idea of the current state-of-the-art on classical computers see, e.g., Ref. [8].

In more complex hydrodynamical problems, other dimensionless numbers are present, for example, the Mach number for compressible turbulence, and/or the magnetic Reynolds number for Magnetohydrodynamic (MHD) turbulence, thereby contributing to an even more challenging computational problem.

It is therefore not surprising that the possibility of performing quantum simulations of fluid and plasma dynamics has already attracted considerable attention [9–19]. In essence, the methods investigated so far include (i) the quantum amplitude estimation algorithm to solve a discretized Navier-Stokes equation [9], (ii) standard form encoding combined with quantum walks to simulate a lattice Boltzmann approach [10], (iii) the quantum Fourier transform to implement vortex-in-cell methods [11–13], (iv) working with multiple copies of each state to implement nonlinearity [14], (v) truncation and linearization methods to simplify nonlinear terms [15–17], and (vi) extending configuration space [18].

The aim of this paper is to present a manner of simulating both relativistic and nonrelativistic quantum fluids on existing and future quantum computers.

The Dirac equation [20] plays a pivotal role in this approach. On one hand, the Dirac equation can be mapped into relativistic hydrodynamics by a generalization of the so-called Madelung transformation initially developed for the Schrödinger equation [21,22] and later extended to the Klein-Gordon (KG) equation [23–25] and quaternionic quantum mechanics [26]. On the other hand, quantum walks, which can be viewed as a quantum generalization of classical random walks [27–30], are a universal quantum primitive [31,32]; every quantum algorithm can be expressed as a quantum walk, and several quantum walks, usually called Dirac quantum walks, admit the Dirac equation as continuous limit [33,34]. The Dirac equation can therefore be used as a bridge connecting relativistic fluid dynamics to quantum walks and, thus, to quantum simulation and quantum computing.

To make the presentation definite and keep it as simple as possible, we restrict ourselves to fluids moving in $(1+1)$ dimensional space-time. Having future applications to extreme,i.e., both relativistic and quantum plasmas in mind, we allow the fluid to be charged and experience an imposed but not necessarily constant or uniform electric field [there is no magnetic field in $(1+1)$ dimensions]. We therefore introduce a generalization of the Madelung transformation which maps the *charged* Dirac equation unto the hydrodynamics of a *charged* relativistic quantum fluid, focusing on the conserved quantities,i.e., charge and energy momentum. Simulating quantum relativistic flows of this fluid can then be carried out by simulating the Dirac dynamics through Dirac quantum walks.

In practice, the quantum walks are defined at all times of interest on a spatial grid of N points and are composed of two steps per time: a shift operation and a mix operation. It is convenient to work in Fourier space where the shift operation is easier to implement. Performing a Fourier transform on a set of $N = 2^n$ data requires $O(N \log N)$ operations using the fast Fourier transform (FFT) algorithm [35], which poses exponential-in-n requirements on the amount of classical memory needed to perform the computation. On a quantum computer, the data can be stored in n qubits and the Fourier transform can be efficiently implemented using the quantum Fourier transform (QFT) algorithm, which needs only $O(n^2)$ operations [36,37] (the QFT can even be approximately implemented using $O(n \log n)$ operations [38]). Indeed, a quantum circuit on n qubits can be said efficient when the total number of primitive quantum gates to approach a given unitary $\hat{U}$ with precision ϵ scales at worst as $O(\text{poly}(n, \frac{1}{\epsilon}))$. Basic quantum walks can be efficiently implemented on a universal quantum computer since the mix operation corresponds to a single quantum gate [39].

Unfortunately, full-fledged circuit-based quantum computers do not exist, yet so no direct quantum numerical simulation of quantum relativistic fluids can be performed today. We nevertheless present, as an illustration, classical and NISQ-based hybrid simulations in the simple situation where the electric field E is uniform, using the gauge where E is entirely encoded in the time dependence of the vector potential. The different Fourier components then evolve independently of each other. It is then possible to quantum simulate each wave number separately on the maximum number of qubits which allow us to perform fault-tolerant computations. The simulation is hybrid because the Fourier transform is carried out classically.

Both the classical and NISQ simulations that we present here are focused on shocks. There are several reasons for this. First, shocks correspond to (near) discontinuities appearing in the velocity field, and are thus notoriously difficult to simulate. Also, the precise, so-called internal structure of shocks is an important topic in theoretical hydrodynamics and statistical physics, especially in the relativistic context (see, for example, Refs. [40,41] for an introduction to this and related topics). Third, shocks are very important in practice. They are generated, for example by, supersonic flight and are also the seed for important astrophysical phenomena [42].

The final section sums up our results and discusses possible extensions to other fluids, both classical and quantum, with possible coupling to arbitrary Yang-Mills and gravitational fields. Applications include, in particular, electromagnetic and quark-gluon plasma dynamics, both for earth-based and astrophysical problems. The nonrelativistic limit of our results is discussed in the Appendix. The general conclusion of this paper is that quantum walks can be used to simulate nonlinear hydrodynamics on future quantum computers.

II. CHARGED DIRAC FLUID

It is well-known that the Schrödinger equation can be cast into a hydrodynamic form through the so-called Madelung transformation [21,22]. The Dirac equation admits a charge current and a stress-energy tensor, as all charged fluids do. The Madelung transformation for the Dirac equation is best obtained by rewriting the Dirac charge current and stress-energy tensor in terms of standard fluid variables. The Madelung transformation for the $(1+1)$D Dirac equation without electric field has been presented in Ref. [43]. We now demonstrate how those results can be extended to situations where the charged $(1+1)$D Dirac field is coupled to a nonvanishing electric field.

A. Dirac equation

In $(1+1)$D flat space-time, the Dirac equation obeyed by the two component wave function $\psi = (\psi^L, \psi^R)^T$ of a spin $1/2$ field can be written in the form

$$(i\gamma^0 D_0 + i\gamma^1 D_1)\psi - m\psi = 0, \tag{1}$$

where $D_0 = \partial_t + iqA_0$, $D_1 = \partial_x + iqA_1$ and $\gamma^0 = \sigma_X = \left(\begin{smallmatrix} 0 & 1 \\ 1 & 0, \end{smallmatrix}\right)$, $\gamma^1 = i\sigma_Y = \left(\begin{smallmatrix} 0 & 1 \\ -1 & 0 \end{smallmatrix}\right)$. The mass of the field is m, its charge is q, and (A_0, A_1) are the two components (in units $c = 1, \hbar = 1$) of the vector potential acting on the field. Since we are working in $(1+1)$D space-time, there is no magnetic field and the electric field is simply $E = -\partial_x A_0 + \partial_t A_1$.

B. Charge current

The expressions for D_0 and D_1 entering the Dirac equation above make clear that, geometrically speaking, the potential A_μ, with $\mu = 0, 1$, is a connection ensuring the

invariance of the Dirac equation under arbitrary local phase translations. More precisely, Eq. (1) is invariant under the transformation $\psi(t,x) \to \exp(iq\alpha)\psi(t,x)$, $A_0(t,x) \to A_0(t,x) - \partial_t\alpha$, and $A_1(t,x) \to A_1(t,x) - \partial_x\alpha$, where $\alpha(t,x)$ is an arbitrary function of time and space. This invariance implies, through Noether's theorem, the conservation equation for the charge current J with components $J^0 = q\bar{\psi}\gamma^0\psi$ and $J^1 = q\bar{\psi}\gamma^1\psi$, where $\bar{\psi} = \psi^\dagger\gamma^0$, which reads

$$\partial_t J^0 + \partial_x J^1 = 0. \tag{2}$$

According to standard relativistic hydrodynamics, the charge current J can be expressed in terms of the scalar density n and the two-velocity of the fluid by the simple relation $J = qnu$ or, equivalently, $nu = J/q = j$. Since u is normalized to unity, this relation translates into $n = (j.j)^{1/2}$ and $u = j/(j.j)^{1/2}$ where a dot denotes the Minkovski scalar product. In an arbitrary reference frame, the current j decomposes into the fluid density $\rho = j^0$ in that frame, and into the spatial current density $\rho v = j^1$ in the same frame. The density ρ in the proper frame of the space-time grid on which the walk is defined thus coincides, as it should, with $|\psi^L|^2 + |\psi^R|^2$. Note that ρ coincides with n in the local proper frame of the fluid/Dirac field.

C. Energy momentum

The energy-momentum distribution of the $(1+1)$D Dirac field in the presence of the electromagnetic field A is described by its stress-energy tensor T, which reads $T^{\mu\nu} = \frac{i}{4}(\bar{\psi}\gamma^\mu\partial^\nu\psi - \partial^\nu\bar{\psi}\gamma^\mu\psi) - \frac{1}{2}A^\mu J^\nu + (\mu \leftrightarrow \nu)$ where J is the conserved charge current. The stress-energy tensor T obeys

$$\partial_\mu T^{\mu\nu} = F^\nu_{\ \mu} J^\mu, \tag{3}$$

where $F^\nu_{\ \mu} = \partial^\nu A_\mu - \partial_\mu A^\nu$ is the electromagnetic tensor. The energy momentum of the Dirac field is *not* conserved because the fluid experiences the force created by the electromagnetic field, and $F^\nu_{\ \mu} J^\mu$ is indeed the density of the Lorentz two-force. In particular $F^1_{\ \mu} J^\mu = q\rho E$ represents the density of the electric force exerted by the electric field on the Dirac field, and $F^0_{\ \mu} J^\mu$ represents the power density of this force.

The other main thermodynamical variable entering the macroscopic description of a relativistic fluid is the scalar enthalpy density w. Identifying w in terms of wave-function variables is not straightforward. The density w makes the contribution $wu^\mu u^\nu$ to the stress-energy tensor $T^{\mu\nu}$ of a perfect fluid. Considering the stress-energy tensor of the Dirac field leads to the identification $w = mn\cos(\phi_-)$, where $\phi_- = \phi_L - \phi_R$ is the difference between the phases of ψ^L and ψ^R. Using the Dirac equation, the stress energy tensor can then be written as

$$T^{\mu\nu} = wu^\mu u^\nu + \frac{n}{4}\Big[\Big(u^\mu\epsilon^{\nu\alpha} + u^\nu\epsilon^{\mu\alpha}\Big)\partial_\alpha\phi_- + \big(\epsilon^{\mu\alpha}\partial^\nu\phi_- + \epsilon^{\nu\alpha}\partial^\mu\phi_-\big)u_\alpha\Big], \tag{4}$$

where $\epsilon^{\mu\nu}$ is the Levi-Civita completely antisymmetric tensor of rank 2, with the convention $\epsilon^{01} = +1$. The first contribution on the right-hand side is standard for relativistic perfect fluids. The other ones involve derivatives of ϕ_-. Because of the relation between ϕ_- and the enthalpy per particle w/n, one can write

$$d\phi_- = \sigma\frac{1}{m}\Big(1 - \frac{w}{mn}\Big)^{-1/2} d\Big(\frac{w}{n}\Big), \tag{5}$$

where σ is the sign of ϕ_-. Thus, derivatives of ϕ_- can be rewritten as derivatives of the enthalpy per particle and all the terms which follow the perfect fluid part $wu^\mu u^\nu$ in the expression of the stress-energy tensor are therefore generalized quantum pressure terms, whose appearance is expected in the description of quantum fluids [3,21,22].

D. Equations of motion

The Dirac equation can be transcribed in terms of the hydrodynamical variables. One obtains

$$\partial_\mu(qnu^\mu) = 0, \tag{6}$$

$$\frac{w}{n}u^\mu = -\frac{1}{2}\left(\partial^\mu\phi_+ + \sigma\epsilon^{\mu\nu}\frac{1}{m}\left(1 - \frac{w}{mn}\right)^{-1/2}\partial_\nu\left(\frac{w}{n}\right)\right) - qA^\mu, \tag{7}$$

$$\epsilon^\mu_{\ \alpha}\partial_\mu(nu^\alpha) = 2mn\sin(\phi_-), \tag{8}$$

where $\phi_+ = \phi_L + \phi_R$. The first equation is the continuity equation expressing charge conservation. The second equation is a generalization of the standard definition of potential flows for relativistic charged fluids in the presence of an electromagnetic potential A. The phase $\phi_+/2$ plays the role of the standard relativistic velocity potential but there is an extra term involving the derivatives of ϕ_-, which can be expressed in terms of w/n and which actually prevents the flow from being potential. The last equation has no easy interpretation but is needed to form a set of four independent equations for the four independent hydrodynamical variables n, u^1 related to u^0 via $u^0 = \sqrt{1 + (u^1)^2}$, w, and the potential ϕ_+.

III. NONRELATIVISTIC FLOWS

In this section, the Planck's constant and the velocity of light are not equal to unity, i.e., $\hbar \neq 1$, $c \neq 1$, to see more clearly the quantum and relativistic part of the hydrodynamic equations.

The nonrelativistic limit corresponds to a situation where the velocity v of the fluid is much smaller than the velocity of light c, implying that the energy of the particle is almost equal to the remaining mass energy: $E = E' + mc^2$ with $E' \ll mc^2$. The relativistic part of the wave function has to be extracted by writing $\frac{\phi_+}{2} = \phi - mc^2 t$, where we will see that ϕ is the nonrelativistic velocity potential. More details on the limiting procedure can be found in the Appendix. In the nonrelativistic regime, the two components of the wave function become identical and the $(1+1)$D Dirac equation degenerates into a single, one-component Schrödinger equation. Then the relativistic fluid variables and equations defined in the previous section become the usual Madelung transformation of the Schrödinger equation in the presence of electromagnetic fields. The fluid density becomes $n = 2r^2$ with $r = |\psi^L| = |\psi^R|$, while the fluid velocity u^1 becomes the usual generalized velocity $u^1 = v = \frac{1}{m}(\partial_x\phi + qA_1)$. Then the

set of four independent relativistic fluid equations Eqs. (6)–(8) degenerate into a set of two independent fluid equations: one expressing the conservation of matter (or charge) and another the generalization of Bernoulli equation for a potential fluid in an electromagnetic potential $V = cA_0$ and a quantum (Bohm) potential $Q = -\frac{\hbar^2}{2m}\frac{1}{\sqrt{n}}\frac{\partial^2\sqrt{n}}{\partial x^2}$, (which vanishes in the classical limit $\hbar \to 0$):

$$\partial_t n + \partial_x(nv) = 0, \tag{9}$$

$$\partial_t \phi + \tfrac{1}{2}mv^2 + qV + Q = 0. \tag{10}$$

The gradient of this Bernoulli equation leads to the inviscid Burgers' equation for a charged fluid in an electric field $E = -\partial_x V + \partial_t A_1$ and a quantum pressure force $F_Q = -\partial_x Q$:

$$m(\partial_t v + v\partial_x v) = qE + F_Q. \tag{11}$$

IV. QUANTUM WALKS AS DISCRETIZATIONS OF THE DIRAC EQUATION

DTQWs are defined in discrete space and discrete time and have an internal degree of freedom usually called the coin. In this paper, we focus on DTQWs defined in discrete 1D space. Having spectral simulations in mind, we also take space to be N periodic, where N is a power of 2 and we label the grid points by $p \in \mathbf{N}_p = \{-N/2, -N/2+1, \ldots, N/2-1\}$. Discrete instants are labeled by $l \in \mathbf{N}$. We also choose the coin space to be 2D and denote by $(|L\rangle, |R\rangle)$ an arbitrary fixed orthonormal basis in that space. With these conventions, the state of the walk at time l can be written as $|\psi\rangle_l = \sum_p \psi^L_{l,p}|p\rangle|L\rangle + \psi^R_{l,p}|p\rangle|R\rangle$, where the set of complex numbers $\{\psi^L_{l,p}, \psi^R_{l,p}\}$ with $p \in \mathbf{N}_p$ represents the two-component wave function of the walk at time l. At each time step, the walk is advanced through the successive action of two unitary operators, one which acts in position space and one which acts in coin space. The operator $\hat{S}$ acts in position space and is usually called the shift operator; it is defined by $\hat{S} = |L\rangle\langle L| \sum_p |p-1\rangle\langle p| + |R\rangle\langle R| \sum_p |p+1\rangle\langle p|$. The shift operator is thus a coin-conditioned spatial translation which moves every $\psi^L_{l,p}$ to the left by one unit and every $\psi^R_{l,p}$ to the right, also by one unit. The operator $\hat{C}_l$ acting in coin space is allowed to depend on time l and, at each point p, mixes the L and R components in a unitary manner. This operator is defined by $\hat{C}_l = \sum_p \hat{C}_{l,p}|p\rangle\langle p|$ with $\hat{C}_{l,p} = e^{-i\epsilon q(A_0)_{l,p}} R_X(2\epsilon m) R_Z(-2\epsilon q(A_1)_{l,p})$, where $R_X(\theta) = \begin{pmatrix} \cos(\theta/2) & -i\sin(\theta/2) \\ -i\sin(\theta/2) & \cos(\theta/2) \end{pmatrix}$ and $R_Z(\theta) = \begin{pmatrix} e^{-i\theta/2} & 0 \\ 0 & e^{i\theta/2} \end{pmatrix}$ are primitive single qubit operations [36]. The potential vector A_0 and A_1 are arbitrary real numbers, as are the two real positive parameters ϵ and m. It is useful to introduce the notation $\hat{U}_l = \hat{C}_l\hat{S}$, which makes it possible to write the evolution equation of the quantum walks in the compact form $|\psi\rangle_{l+1} = \hat{U}_l|\psi\rangle_l$. The interpretation of these quantities becomes clear in the continuum limit. The continuum limit can be investigated by introducing the space-time coordinates $x_p = \epsilon p$, $t_l = \epsilon l$ and letting ϵ tend to zero [33]. The wave function of the walk then becomes a continuous function of x and t which obeys the Dirac equation introduced earlier.

The current j can be determined from the wave function of the DTQW using the formula $(j^0)_{l,p} = |\psi^R_{l,p}|^2 + |\psi^L_{l,p}|^2$ and $(j^1)_{l,p} = |\psi^R_{l,p}|^2 - |\psi^L_{l,p}|^2$ where l denotes a discrete time coordinate and p a discrete space coordinate. Thus, the fluid density reads $n_{l,p} = \sqrt{(j^0)^2_{l,p} - (j^1)^2_{l,p}} = 2|\psi^L_{l,p}||\psi^R_{l,p}|$ and the fluid velocity normalized to the speed of light c reads $(\frac{u^1}{u_0})_{l,p} = \frac{(j^1)_{l,p}}{(j^0)_{l,p}}$.

V. SIMULATIONS OF DIRAC FLOWS FOR UNIFORM ELECTRIC FIELDS

A. Spectral formulation of the quantum walks

Let E be the constant uniform value of the electric field. To make the computation simpler, we choose the gauge $A_0 = 0$, $(A_1)_l = El\epsilon$, where the vector potential depends only on the discrete time l and so the coin operator $\hat{C}_{l,p} = \hat{C}_l$. The classical and NISQ simulations are accomplished in Fourier space where the shift operator entering the definition of the walks amounts to a coin-controlled multiplication by a phase factor. More precisely, let $\tilde{\psi}_{l,k} = \frac{1}{\sqrt{N}}\sum_{p=-N/2}^{N/2-1} \psi_{l,p} e^{-2i\pi kp/N}$ be the discrete Fourier transform of a function defined on the discrete space-time grid. In Fourier space, the equations of the walk, $\forall l, k \in \mathbf{N} \times \mathbf{N}_p$, read

$$\begin{pmatrix} \tilde{\psi}^L_{l+1,k} \\ \tilde{\psi}^R_{l+1,k} \end{pmatrix} = \hat{C}_l \begin{pmatrix} e^{2i\pi k/N} & 0 \\ 0 & e^{-2i\pi k/N} \end{pmatrix} \begin{pmatrix} \tilde{\psi}^L_{l,k} \\ \tilde{\psi}^R_{l,k} \end{pmatrix}, \tag{12}$$

where the absence of spatial convolution is due to the choice of gauge.

B. The full-quantum algorithm

In recent years, several circuit-based implementation schemes for DTQW have been devised and experimentally realized. A recent implementation has been made on a five-qubit trapped-ion quantum processor [44]. In most cases, DTQWs are implemented by blocks of multicontrolled Toffoli gates, typically of size $O(n^3)$ and depth $O(n^2)$ [45], where n is the number of qubits. Quite interesting is the recent scheme proposed by Shakeel [39], where the basic QWs are formulated in terms of a simple QFT-based circuit [37], polynomially improving the previous results in terms of complexity. Indeed, it yields a highly efficient and scalable, quadratic size, linear depth circuit for the basic DTQW. This algorithm gives the full-quantum circuit needed to perform the simulations on $n+1$ qubits with a coin operator $\hat{C}_l$. We also suppose that the initial state $\psi_0 = \sum_{p\in\mathbf{N}_p} \psi^R_{0,p}|p\rangle|R\rangle + \psi^L_{0,p}|p\rangle|L\rangle$ can be efficiently implemented on the $n+1$ qubits following methods developed in Refs. [46–48]. In this full-quantum algorithm, the quantum advantage is lost if one wants to determine the entire final state after T steps. One can still efficiently measure a finite number (small when compared to 2^n) of averaged values of local and global observables [49–51] such as the energy, the momentum, or the density.

However, this full-quantum algorithm is not NISQ compatible since the performances of the current quantum processors do not allow us to perform a large amount of quantum gates on entangled qubits without too many errors. For instance, recent implementations of quantum walks on NISQ quantum processors have shown significant results for only a very few

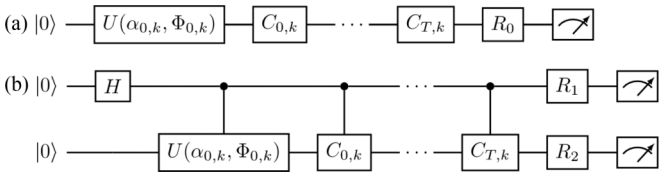

FIG. 1. Quantum part of the NISQ algorithm for DTQW to compute every $|k\rangle_T$.

number of qubits (less than five) and a very few number of steps (less than five) [39,52,53].

C. The NISQ algorithm

We now present a hybrid quantum-classical algorithm based on a discrete time quantum walk (DTQW) discretization of the charged Dirac fluid tailor-made for NISQ devices.

The main idea is to split the quantum operations on sets of qubits which allow us to perform fault-tolerant computations. The minimum number of qubits needed to perform this scheme is two, but it can be increased depending on the performance of the NISQ devices, at the same time increasing the quantum advantage of this method. In the following, we choose to develop the numerical scheme in the limit of sets of two qubits where the errors are small enough to get meaningful results.

The algorithm is composed of two distinct parts. In the first one, we perform the FFT on the initial classical state $\psi_{0,p}$, where p refers to the discrete space $p \in \mathbf{N}_p = \{-N/2, -N/2+1, \ldots, N/2-1\}$ with N a power of 2 to get the Fourier-transformed $\tilde{\psi}_{0,k}$ with $k \in \mathbf{N}_p$. In Fourier space, each $\tilde{\psi}_{l,k}$, with $l \in \mathbf{N}$ the discrete-time coordinate, evolves independently from the others, allowing us to parallelize the computations of each mode on the different sets of qubits. Moreover, $\forall k$, we need to memorize the normalization factor $n(k) = \sqrt{|\tilde{\psi}^L_{0,k}|^2 + |\tilde{\psi}^R_{0,k}|^2}$ and the global phase Φ^+_k for further steps of the algorithm. To apply the quantum circuit, we need to encode the above classical information in a quantum state; this can be done efficiently, as follows. At the beginning, for each mode, the quantum state, represented by a qubit, is set to $|0\rangle$ in the canonical basis. Then, we perform a quantum rotation in the Bloch sphere,

$$|k\rangle_0 = U(\alpha_{0,k}, \Phi^-_{0,k})|0\rangle, \tag{13}$$

where

$$U(\alpha_{0,k}, \Phi^-_{0,k}) = \begin{pmatrix} \cos(\alpha_{0,k}/2) & -\sin(\alpha_{0,k}/2) \\ \sin(\alpha_{0,k}/2)e^{i\Phi^-_{0,k}} & \cos(\alpha_{0,k}/2)e^{i\Phi^-_{0,k}} \end{pmatrix}.$$

The encoded initial quantum state finally reads

$$\tilde{\psi}_{0,k} = n(k)e^{i\Phi^+_{0,k}}|k\rangle_0. \tag{14}$$

As we show in Fig. 1, the total evolution of the walker is achieved by the quantum subroutine (a) by performing one quantum rotation $C_{l,k}$ on each $|k\rangle_0$ [see Eq. (12)]. After T such rotations, the final qubit reads

$$|k\rangle_T = e^{i\Phi^+_{T,k}} \begin{pmatrix} \cos(\alpha_{T,k}/2) \\ \sin(\alpha_{T,k}/2)e^{i\Phi^-_{T,k}} \end{pmatrix}. \tag{15}$$

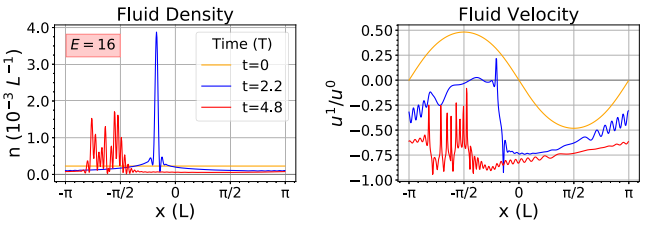

FIG. 2. Profiles of density n (left) and velocity u^1/u^0 (right) at different times as functions of the position x, for an electric field $E = 16$, charge $q = -1$, mass $m = 64$, and initial maximum velocity $u_{\max} = 0.55$. The mesh size is $N = 4096$, $\epsilon = 2\pi/N$, T is an arbitrary time unit and L is an arbitrary length unit.

Finally, the state is successively measured into the x, y, z basis by choosing $R_0 = H, S_1^\dagger H, I_2$, with $H = \frac{1}{\sqrt{2}}\begin{pmatrix} 1 & 1 \\ 1 & -1 \end{pmatrix}$ and $S_1 = \begin{pmatrix} 1 & 0 \\ 0 & i \end{pmatrix}$ and by repeating the procedure until one gets enough statistics to determine the coefficients $\alpha_{T,k}$ and $\Phi^-_{T,k}$. However, to implement the very last step of the algorithm, namely, the inverse FFT, one also needs the global phase $\Phi^+_{T,k}$. This can be done using the quantum circuit (b), where a single qubit controls the $C_{l,k}$ rotations, allowing us in the end to measure the global phase by choosing $R_1 = H, S_1^\dagger H$ and $R_2 = I_2$. Finally, we can perform the classical inverse FFT on

$$\tilde{\psi}_{T,k} = n(k)e^{i(\Phi^+_{0,k}+\Phi^+_{T,k})} \begin{pmatrix} \cos(\alpha_{T,k}/2) \\ \sin(\alpha_{T,k}/2)e^{i\Phi^-_{T,k}} \end{pmatrix} \tag{16}$$

to obtain the final state of the quantum walk $\psi_{T,p}$.

D. Simulations on IBM quantum processors

Simulations have been performed on classical processors (Figs. 2 and 3) and on IBM's publicly available quantum processors (Figs. 4 and 5). The initial condition of the quantum walk is chosen such as to obtain hydrodynamical shocks: the initial fluid density n is constant, while the initial fluid velocity u^1/u^0 is antisymmetric with respect to $x = 0$.

More precisely, let us note $\psi(x,t) = e^{i\phi_+/2}\begin{pmatrix} |\psi^L|e^{i\phi_-/2} \\ |\psi^R|e^{-i\phi_-/2} \end{pmatrix}$ with $|\psi^L| = \frac{1}{\sqrt{2}}\sqrt{j^0 - j^1}$ and $|\psi^R| = \frac{1}{\sqrt{2}}\sqrt{j^0 + j^1}$. To get a shock we need an anti-symmetric initial velocity u^1/u^0, thus we choose a global phase $\phi_+ = 2mu_{\max}\cos(x)$ with max a positive number and a relative phase $\phi_- = 0$. Equation (7) implies that $j^1 = -nu_{\max}\sin(x)$, and so $u^1 = -u_{\max}\sin(x)$. Then $j^0 = +\sqrt{n^2 + (j^1)^2} = n\sqrt{1 + (u_{\max}\sin(x))^2}$ and, finally, $u^1/u^0 = j^1/j^0$ is antisymmetric. The fluid density can be an arbitrarily chosen constant; we set $n = 1$. This initial condition is inspired by similar choices used to simulate the dynamics of a nonquantum cosmological fluid [54], Bose-Einstein condensates of axions [55], and quantum walk hydrodynamics [43].

In Fig. 2, the fluid density and velocity are displayed at three different times. The shock is characterized by a peak in the fluid density n and a small region with a large gradient in the fluid velocity u^1/u^0 at $t = 2.2$. After the impact, the front of the shock propagates to the left due to the external electric field, yielding a nontrivial shock structure at $t = 4.8$. Figure 3 shows the fluid density and velocity with respect to space and time for several values of the electric field.

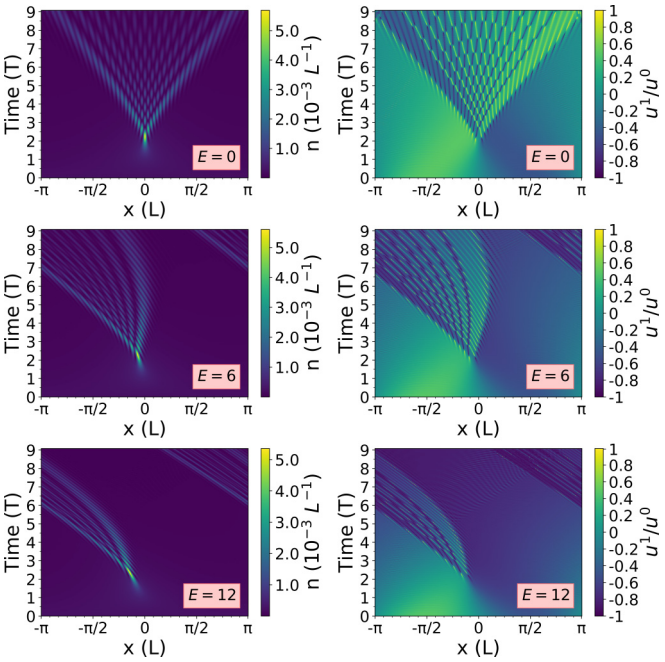

FIG. 3. Evolution of the shock's density n (left) and velocity u^1/u^0 (right) as functions of the position x and time for different values of the electric field $E = 0, 6, 12$, charge $q = -1$, mass $m = 64$, and initial maximum velocity $u_{\max} = 0.55$. The mesh size is $N = 4096$, $\epsilon = 2\pi/N$, T is an arbitrary time unit, and L is an arbitrary length unit.

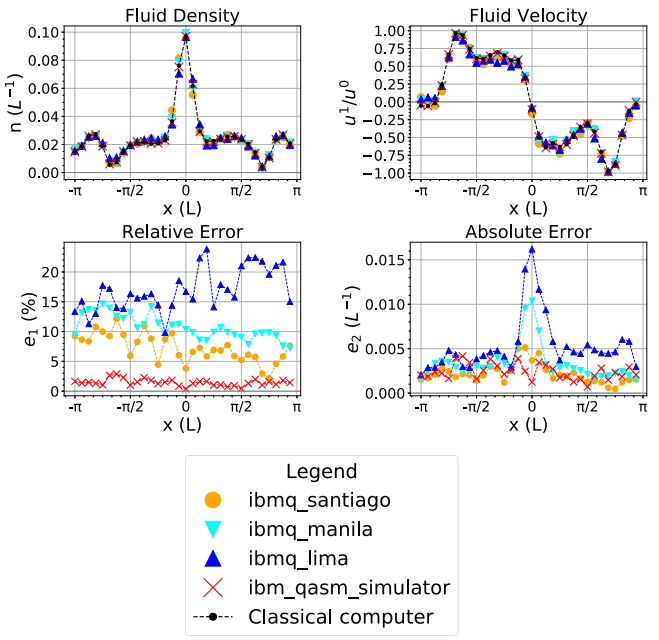

FIG. 4. Shock's profiles of fluid density n (upper left) and fluid velocity u^1/u^0 (upper right) as functions of position x computed on different IBM's quantum processors, `ibm_qasm_simulator` and a classical computer, at $t = 1.96$ (arbitrary unit). The lower panels show relative errors (lower left) and absolute error (lower right) between the ideal results obtained on the classical computer and the results obtained on the quantum processors and simulator. The simulation parameters are electric field $E = 0.6$, charge $q = -1$, mass $m = 6$, and initial maximum velocity $u_{\max} = 0.92$. The mesh size is $N = 32$, $\epsilon = 2\pi/N$, and L is an arbitrary length unit.

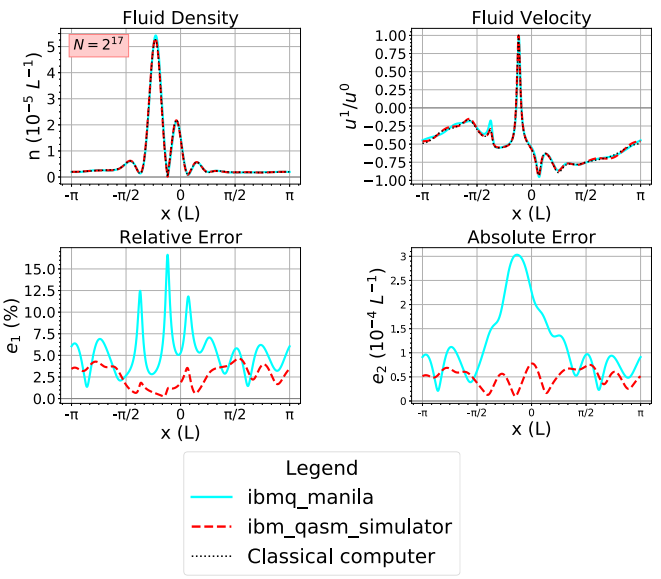

FIG. 5. High-resolution shock's profiles of fluid density n (upper left) and fluid velocity u^1/u^0 (upper right) computed on `ibmq_manila` quantum processor, `ibm_qasm_simulator`, and classical computer at $t = 2.5$ (arbitrary unit), with $N = 2^{17}$ grid points, an electric field $E = 2$, a charge $q = -1$, a mass $m = 6$, an initial maximum velocity $u_{\max} = 0.92$, $\epsilon = 2\pi/N$, L an arbitrary length unit, relative errors (lower left), and absolute error (lower right) between the ideal results obtained on a classical computer and the results obtained on quantum processors and simulator as functions of the position x.

The shocks are perfectly symmetric around $x = 0$ in the absence of electric field. For nonvanishing electric fields, the shocks are accelerated in the direction of the field. These results have been successfully recovered using IBM's quantum processors. Figure 4 shows the first simulations of hydrodynamical shocks using NISQ devices on a line of $N = 32$ nodes. The same simulation has been performed on three different quantum processors (`ibmq_santiago`, `ibmq_manila`, `ibmq_lima`) and the results are compared with a simulator of quantum devices (`ibm_qasm_simulator`) and a classical computer. The performances of the different IBM's quantum processors are compared with the relative error defined as

$$e_1 = 100\frac{\sqrt{\left|\psi^L_{x,q} - \psi^L_{x,c}\right|^2 + \left|\psi^R_{x,q} - \psi^R_{x,c}\right|^2}}{\sqrt{\left|\psi^L_{x,c}\right|^2 + \left|\psi^R_{x,c}\right|^2}}, \tag{17}$$

and the absolute error defined as

$$e_2 = \sqrt{\left|\psi^L_{x,q} - \psi^L_{x,c}\right|^2 + \left|\psi^R_{x,q} - \psi^R_{x,c}\right|^2}, \tag{18}$$

where q refers to the quantum devices and simulator and c to the classical computer. Even if the relative errors range from 3% to 24%, the results on the fluid density and velocity are qualitatively accurate, showing the expected shock. The finite number of measurements $M = 8096$ leads to statistical errors of the order of 3% as shown by the relative errors of `ibm_qasm_simulator`. Figure 5 shows the results obtained on a grid of $N = 2^{17}$ points with the `ibmq_manila` quantum processor showing first that this hybrid algorithm allows us

to perform large simulations on NISQ devices. The velocity almost reaches the speed of light $u^1/u^0 \approx 0.9993$ at $x \approx -\frac{3\pi}{24}$ where the density n almost vanishes, proving ultrarelativistic behavior in the shocks.

Let us conclude this section with two remarks. Before any computation on its quantum processors, IBM automatically transpiles the quantum circuit to reduce the number of primitive quantum operations and the errors. However, the transpiler does not perform efficiently in the case of circuit (b) presented Fig. 1, giving completely noisy results. We found that this difficulty can be overcome if we transpile the quantum circuit (a) before transpiling the control-circuit (a) which is contained in circuit (b).

The second remark relates to Fig. 5. The simulation on a grid of $N = 2^{17}$ points has been successfully performed thanks to a compression of the wave function in Fourier space. Indeed, the momentum is bounded by the quantity $mu_{\max}$ and the Fourier space is discretized with a step $\Delta k = \frac{2\pi}{N\Delta x}$. By choosing $\Delta x = \frac{2\pi}{N}$, then $\Delta k = 1$ and most of the Fourier components of the DTQW vanishes for $k > k_{\max} = mu_{\max}$ ($\hbar = 1, c = 1$), reducing drastically the computations.

VI. SUMMARY AND DISCUSSION

A. Summary

We have shown that present-day IBM's NISQ devices can simulate quantum-relativistic-charged fluids in an electric field. Our approach is based on a hybrid classical-quantum algorithm using DTQW with continuous-limit Dirac equation mapped into relativistic hydrodynamics by a generalization of the Madelung transformation. We have also discussed several extensions which may reasonably be carried out with success in the near future. These include nonquantum fluids and fluids coupled to arbitrary gauge fields. All in all, this paper opens the door to more efficient quantum simulation of quantum and classical hydrodynamics [56,57], with natural applications to quantum, possibly relativistic plasmas [58–60].

B. Discussion

Let us now discuss the results presented in this paper, focusing in particular on possible extensions.

All the results presented above address hydrodynamics in $(1 + 1)$ space-time dimensions, and should therefore be extended to higher dimensions. We believe this extension should be possible but is non-trivial either because (i) the number of spinor components depends on the space-time dimension (e.g,. a spinor in $(1 + 3)$ dimensions), and (ii) the Madelung transformation for a non-charged Dirac fluid is much simpler in $(1 + 1)$ dimensions than in higher dimensions.

In higher dimensions, a charged fluid can be coupled not only to electric fields but also to magnetic ones. Moreover, these fields may not be uniform and constant, as is the electric field considered in this paper. More generally, Dirac particles and their discrete counterparts,i.e., DTQWs, can also be coupled to arbitrary Yang-Mills gauge field [61,62] and relativistic gravitational fields [63–65]. Extending the above results in these directions would, for example, open up the possibility of simulating quark-gluon plasmas and extreme astrophysical plasmas on hybrid quantum-classical computers. DTQWs can also be used as a basis to build full-fledged discrete gauge theories. Can the hybrid algorithm presented above be extended to simulate these discrete gauge theories? If so, the extension would make it possible to simulate not only fluids in external, imposed gauge fields but also self-consistent problems where the dynamics of the gauge fields and the fluids are fully coupled, as in self-consistent plasma dynamics.

Finally, the hybrid algorithm we propose should be extended to quantum and classical fluids with other equations of state. The key is to consider more general quantum walks and quantum automata. Self-interacting walks and automata [66–68] are of particular interest because they are a relatively easy tool to model arbitrary equations of state and because several implementations of QCAs have been suggested, including Rydberg states [69]. Also, general equations of state can, in principle, be implemented by using a quantum information device as a quantum system with effective nonlinear dynamics like Bose condensates [70,71].

ACKNOWLEDGMENTS

N.F.L. was partially funded by Award No. DE-SC0020264 from the U.S. Department of Energy. We acknowledge the use of IBM Quantum services for this work. The views expressed are those of the authors and do not reflect the official policy or position of IBM or the IBM Quantum team.

The authors declare no competing interests.

APPENDIX: NONRELATIVISTIC LIMIT

1. Dirac equation

The Dirac equation $i\gamma^\mu D_\mu \psi - m\psi = 0$ reads, in component terms and in units where $\hbar \neq 1$ $c \neq 1$:

$$\frac{1}{c}\left(\partial_t + i\frac{qV}{\hbar}\right)\Psi^L - \left(\partial_x + i\frac{qA_1}{\hbar}\right)\Psi^L = -i\frac{\mathrm{mc}}{\hbar}\Psi^R,$$
$$\frac{1}{c}\left(\partial_t + i\frac{qV}{\hbar}\right)\Psi^R + \left(\partial_x + i\frac{qA_1}{\hbar}\right)\Psi^R = -i\frac{\mathrm{mc}}{\hbar}\Psi^L. \quad \text{(A1)}$$

Each component obeys the same KG equation,

$$\frac{1}{c^2}D_{tt}\Psi^{L/R} - D_{xx}\Psi^{L/R} = -\frac{m^2c^2}{\hbar^2}\Psi^{L/R}, \quad \text{(A2)}$$

where $D_{tt} = (D_t)^2 = (\partial_t + i\frac{qV}{\hbar})^2$ and $D_{xx} = (D_x)^2 = (\partial_x + i\frac{qA_1}{\hbar})^2$.

To determine the nonrelativistic limit, we have to extract out the relativistic part of the wave function as $\Psi^{L/R} = \bar{\Psi}^{L/R}\exp(-i\frac{\mathrm{mc}^2}{\hbar}t)$ and consider $\bar{\Psi}^{L/R}$ as the wave function of the particle in the nonrelativistic limit. The nonrelativistic energy of the particle is $E' = E - \mathrm{mc}^2$ with $E' \ll \mathrm{mc}^2$. We therefore expect that $|\frac{\partial\bar{\Psi}^{L/R}}{\partial t}| \sim |\frac{E'}{\hbar}\bar{\Psi}^{L/R}| \ll \frac{\mathrm{mc}^2}{\hbar}|\bar{\Psi}^{L/R}|$, $|\frac{\partial\bar{\Psi}^{L/R}}{\partial x}| \sim |k\bar{\Psi}^{L/R}| = |\frac{p}{\hbar}\bar{\Psi}^{L/R}| \ll \frac{\mathrm{mc}}{\hbar}|\bar{\Psi}^{L/R}|$. The limit only works if the potential A_μ is weak,i.e., $|qA_\mu| \ll \mathrm{mc}$ for $\mu = 0, 1$. We define the dimensionless slow variables $X = \nu(\frac{\mathrm{mc}}{\hbar})x$ and $T = \nu^2(\frac{\mathrm{mc}^2}{\hbar})t$, where ν is a positive real number. The nonrelativistic limit is recovered by letting ν tend to zero while keeping $\partial_X\bar{\Psi}^{L/R} = O(1)$, $\partial_T\bar{\Psi}^{L/R} = O(1)$, $\frac{V}{\nu^2} = O(1)$, and $\frac{A_1}{\nu} = O(1)$.

Injecting the above scaling in the KG equation for $\bar{\Psi}_{L/R}$ shows that $\bar{\Psi}_{L/R}$ both obey the Schrödinger equation with electromagnetic fields when ν goes to zero. We now also compute for future use the lowest order terms in the difference $\bar{\Psi}_L - \bar{\Psi}_R$. The Dirac equation can be rewritten as

$$\begin{aligned}\bar{\Psi}_R &= \bar{\Psi}_L - i\nu D_X \bar{\Psi}_L + i\nu^2 D_T \bar{\Psi}_L + O(\nu^3),\\ \bar{\Psi}_L &= \bar{\Psi}_R + i\nu D_X \bar{\Psi}_R + i\nu^2 D_T \bar{\Psi}_R + O(\nu^3),\end{aligned} \tag{A3}$$

with $D_X = \partial_X + i\frac{qA_1}{\mathrm{mc}\nu}$ and $D_T = \partial_T + i\frac{qV}{\mathrm{mc}^2\nu^2}$.

Using the Schrödinger equation to replace the temporal derivatives by spatial derivatives leads to

$$\begin{aligned}\bar{\Psi}_R &= \bar{\Psi}_L - i\nu D_X \bar{\Psi}_L - \frac{\nu^2}{2} D_{XX} \bar{\Psi}_L + \mathcal{O}(\nu^3),\\ \bar{\Psi}_L &= \bar{\Psi}_R + i\nu D_X \bar{\Psi}_R - \frac{\nu^2}{2} D_{XX} \bar{\Psi}_R + O(\nu^3).\end{aligned} \tag{A4}$$

Let us start the discussion by keeping only the terms of order ν in Eq. (A4). The two wave-function components are equal at order 0 in ν and thus, at this order, have the same moduli and phases. We want to compute the differences between the moduli and the differences between the phases at first order in ν. This is best done in the following way.

Write $\bar{\Psi}_L = r\exp(\frac{i}{\hbar}\phi)$ and $\bar{\Psi}_R = (r+\delta r)\exp(\frac{i}{\hbar}(\phi+\delta\phi))$. Inserting this into Eq. (A4) and keeping only first-order terms leads to

$$r\exp(\frac{i}{\hbar}\phi)\left(\frac{i}{\hbar}\delta\phi + \frac{\delta r}{r}\right) = -i\nu D_X \bar{\Psi}_L, \tag{A5}$$

from which one gets

$$\delta\phi = -\frac{\hbar}{2r^2}\nu(\bar{\Psi}_L^* D_X \bar{\Psi}_L + (D_X\bar{\Psi}_L)^*\bar{\Psi}_L). \tag{A6}$$

The difference δr can be obtained in the same manner:

$$\frac{\delta r}{r} = \frac{i}{2r^2}\nu(\bar{\Psi}_L^* D_X \bar{\Psi}_L - (D_X\bar{\Psi}_L)^*\bar{\Psi}_L). \tag{A7}$$

This transcribes into

$$\delta\phi = -\nu\frac{\hbar}{r}\frac{\partial r}{\partial X} \tag{A8}$$

and

$$\frac{\delta r}{r} = \nu\pi, \tag{A9}$$

with $\pi = \frac{1}{\hbar}\frac{\partial\phi}{\partial X} + \frac{qA_1}{\mathrm{mc}\nu}$.

It is straightforward (but tedious) to compute in the same manner the differences in moduli and phases at second order in ν. One finds

$$\delta\phi = -\nu\frac{\hbar}{r}\frac{\partial r}{\partial X} - \frac{\hbar}{2}\nu^2\frac{\partial\pi}{\partial X} \tag{A10}$$

and

$$\frac{\delta r}{r} = \nu\pi + \frac{1}{2}\nu^2\left(\pi^2 + \frac{1}{r^2}\left(\left(\frac{\partial r}{\partial X}\right)^2 - r\frac{\partial^2 r}{\partial X^2}\right)\right).$$

2. Hydrodynamical variables

In the main text, the Dirac wave function is defined as

$$\psi = \frac{1}{\sqrt{2}}e^{\frac{i}{\hbar}\phi_+/2}\begin{pmatrix}\sqrt{j^0 - j^1}\,e^{\frac{i}{\hbar}\phi_-/2}\\ \sqrt{j^0 + j^1}\,e^{-\frac{i}{\hbar}\phi_-/2}\end{pmatrix}. \tag{A11}$$

Thus, the definitions above lead to $\phi_+ = 2\phi + \delta\phi - 2\mathrm{mc}^2 t$ and $\phi_- = -\delta\phi$.

At second order in ν, the hydrodynamical variables defined in the main text read

$$n = 2r^2 + 2r^2\nu\pi + \nu^2 r^2\pi^2 + \nu^2\left(\left(\frac{\partial r}{\partial X}\right)^2 - r\frac{\partial^2 r}{\partial X^2}\right), \tag{A12}$$

$$u^0 = c\left(1 + \frac{1}{2}\nu^2\pi^2\right), \tag{A13}$$

$$u^1 = c\left(\nu\pi + \frac{1}{2r^2}\nu^2\left(\left(\frac{\partial r}{\partial X}\right)^2 - r\frac{\partial^2 r}{\partial X^2}\right)\right), \tag{A14}$$

$$w = \mathrm{mc}^2\left(2r^2 + 2r^2\nu\pi + \nu^2\left(r^2\pi^2 - r\frac{\partial^2 r}{\partial X^2}\right)\right). \tag{A15}$$

3. Hydrodynamical equations

In units where $\hbar \neq 1$ and $c \neq 1$, the relativistic fluid equations can be written as

$$\frac{1}{c}\partial_t(nu^0) + \partial_x(nu^1) = 0, \tag{A16}$$

$$\frac{w}{nc}u^0 = -\frac{\hbar c}{2}\left(\frac{1}{c}\partial_t\phi_+ + \partial_x(\phi_-)\right) - qV, \tag{A17}$$

$$\frac{w}{nc}u^1 = \frac{\hbar c}{2}\left(\partial_x\phi_+ + \frac{1}{c}\partial_t(\phi_-)\right) + qA_1 c, \tag{A18}$$

$$\frac{1}{c}\partial_t(nu^1) + \partial_x(nu^0) = -2\frac{\mathrm{mc}^2}{\hbar}n\sin(\phi-). \tag{A19}$$

By injecting the previous hydrodynamical variables in these equations, one can determine their nonrelativistic limit. The set of four independent hydrodynamical relativistic equations become a set of two independent equations in the nonrelativistic limit at second order in ν:

$$\frac{\partial}{\partial T}(2r^2) + \frac{\partial}{\partial X}(2r^2\pi) = 0, \tag{A20}$$

$$\frac{1}{\hbar}\frac{\partial\phi}{\partial T} + \frac{1}{2}\pi^2 + \frac{qV}{\mathrm{mc}^2\nu^2} - \frac{1}{2\sqrt{2r^2}}\frac{\partial^2\sqrt{2r^2}}{\partial X^2} = 0. \tag{A21}$$

Then, in the normal x and t variables, one gets the continuity equation and the Bernoulli equation of an inviscid fluid of density $n = 2r^2$ and velocity $v = \frac{1}{m}(\partial_x\phi + qA_1)$ in an electromagnetic potential V and a quantum potential

$Q = -\frac{\hbar^2}{2m}\frac{1}{\sqrt{n}}\frac{\partial^2\sqrt{n}}{\partial x^2}$ called the Bohm potential, which vanishes in the nonquantum limit $\hbar \to 0$:

$$\partial_t(n) + \partial_x(nv) = 0, \tag{A22}$$

$$\partial_t(\phi) + \tfrac{1}{2}mv^2 + qV + Q = 0. \tag{A23}$$

The gradient of this Bernoulli equation leads to the nonlinear inviscid Burger equation for a charged fluid in an electric field $E = -\partial_x V + \partial_t A_1$ and a quantum pressure force $F_Q = -\partial_x Q$:

$$m(\partial_t v + v\partial_x v) = qE + F_Q. \tag{A24}$$

[1] R. P. Feynman, Simulating physics with computers, Int. J. Theor. Phys. **21**, 467 (1982).

[2] R. E. Wyatt, *Quantum Dynamics with Trajectories: Introduction to Quantum Hydrodynamics* (Springer Science & Business Media, New York, 2005), Vol. 28.

[3] R. J. Donnelly, *Quantized Vortices in Helium II* (Cambridge University Press, Cambridge, 1991).

[4] N. P. Proukakis and B. Jackson, Finite-temperature models of Bose–Einstein condensation, J. Phys. B: At. Mol. Opt. Phys. **41**, 203002 (2008).

[5] B. Ripperda, F. Bacchini, O. Porth, E. R. Most, H. Olivares, A. Nathanail, L. Rezzolla, J. Teunissen, and R. Keppens, General-relativistic resistive magnetohydrodynamics with robust primitive-variable recovery for accretion disk simulations, Astrophys. J., Suppl. Ser. **244**, 10 (2019).

[6] D. A. Uzdensky and S. Rightley, Plasma physics of extreme astrophysical environments, Rep. Prog. Phys. **77**, 036902 (2014).

[7] U. Frisch and A. N. Kolmogorov, *Turbulence: The Legacy of AN Kolmogorov* (Cambridge University Press, Cambridge, 1995).

[8] K. P. Iyer, K. R. Sreenivasan, and P. K. Yeung, Scaling exponents saturate in three-dimensional isotropic turbulence, Phys. Rev. Fluids **5**, 054605 (2020).

[9] F. Gaitan, Finding flows of a Navier-Stokes fluid through quantum computing, npj Quantum Inf. **6**, 61 (2020).

[10] L. Budinski, Quantum algorithm for the Navier-Stokes equations by using the streamfunction-vorticity formulation and the lattice Boltzmann method, International J. Quantum Inform. **20**, 2150039 (2022).

[11] R. Steijl and G. N. Barakos, Parallel evaluation of quantum algorithms for computational fluid dynamics, Comput. Fluids **173**, 22 (2018).

[12] R. Steijl, Quantum algorithms for fluid simulations, in *Advances in Quantum Communication and Information* (IntechOpen Limited, United Kingdom, 2019), p. 31.

[13] R. Steijl, *Quantum Algorithms for Nonlinear Equations in Fluid Mechanics* (IntechOpen, London, 2020).

[14] S. Lloyd, G. De Palma, C. Gokler, B. Kiani, Z.-W. Liu, M. Marvian, F. Tennie, and T. Palmer, Quantum algorithm for nonlinear differential equations, arXiv:2011.06571.

[15] J.-P. Liu, H. Ø. Kolden, H. K. Krovi, N. F. Loureiro, K. Trivisa, and A. M. Childs, Efficient quantum algorithm for dissipative nonlinear differential equations, Proc. Natl. Acad. Sci. **118**, e2026805118 (2021).

[16] A. Engel, G. Smith, and S. E. Parker, Quantum algorithm for the Vlasov equation, Phys. Rev. A **100**, 062315 (2019).

[17] I. Y. Dodin and E. A. Startsev, On applications of quantum computing to plasma simulations, Phys. Plasmas **28**, 092101 (2021).

[18] P. Love, On quantum extensions of hydrodynamic lattice gas automata, Condensed Matter **4**, 48 (2019).

[19] E. Ye and N. F. G. Loureiro, A quantum-inspired method for solving the Vlasov-Poisson equations, arXiv:2205.11990 (2022).

[20] P. A. M. Dirac and R. H. Fowler, The quantum theory of the electron, Proc. R. Soc. London, Ser. A **117**, 610 (1928).

[21] E. Madelung, Eine anschauliche deutung der Gleichung von Schrödinger [English translation: A revealing interpretation of the Schrodinger equation], Naturwissenschaften **14**, 1004 (1926).

[22] E. Madelung, Quantentheorie in hydrodynamischer form [English translation: Quantum theory in hydrodynamical form], Z. Phys. **40**, 322 (1927).

[23] C. Y. Wong, Klein-Gordon equation in hydrodynamical form, J. Math. Phys. **51**, 122304 (2010).

[24] F. Debbasch and M. E. Brachet, Relativistic hydrodynamics of semiclassical quantum fluids, Physica D **82**, 255 (1995).

[25] F. Debbasch and M. E. Brachet, Non-linear acoustics in Galilean and relativistic barotropic fluids, Physica D **108**, 135 (1997).

[26] P. Love and B. Boghosian, Quaternionic Madelung transformation and non-Abelian fluid dynamics, Physica A **332**, 47 (2004).

[27] Y. Aharonov, L. Davidovich, and N. Zagury, Quantum random walks, Phys. Rev. A **48**, 1687 (1993).

[28] S. Boettcher, S. Falkner, and R. Portugal, Relation between random walks and quantum walks, Phys. Rev. A **91**, 052330 (2015).

[29] R. Portugal, *Quantum Walks and Search Algorithms* (Springer, New York, 2013), Vol. 19.

[30] S. E. Venegas-Andraca, Quantum walks: A comprehensive review, Quant. Info. Proc. **11**, 1015 (2012).

[31] A. M. Childs, Universal Computation by Quantum Walk, Phys. Rev. Lett. **102**, 180501 (2009).

[32] N. B. Lovett, S. Cooper, M. Everitt, M. Trevers, and V. Kendon, Universal quantum computation using the discrete-time quantum walk, Phys. Rev. A **81**, 042330 (2010).

[33] G. Di Molfetta, M. Brachet, and F. Debbasch, Quantum walks in artificial electric and gravitational fields, Physica A **397**, 157 (2014).

[34] J. Zylberman and F. Debbasch, Dirac spatial search with electric fields, Entropy **23**, 1441 (2021).

[35] H. J. Nussbaumer, *The Fast Fourier Transform* (Springer, Berlin, 1981).

[36] M. A. Nielsen and I. Chuang, *Quantum Computation and Quantum Information* (American Association of Physics Teachers, 2002).

[37] D. Coppersmith, An approximate Fourier transform useful in quantum factoring, arXiv:quant-ph/0201067.

[38] L. Hales and S. Hallgren, An improved quantum Fourier transform algorithm and applications, in *Proceedings 41st Annual Symposium on Foundations of Computer Science* (IEEE, New York, 2000), pp. 515–225.

[39] A. Shakeel, Efficient and scalable quantum walk algorithms via the quantum Fourier transform, Quant. Info. Proc. **19**, 323 (2020).

[40] W. Israel, Covariant fluid mechanics and thermodynamics: An introduction, in *Relativistic Fluid Dynamics*, edited by A. Anile and Y. Choquet-Bruhat, Lecture Notes in Mathematics, Vol. 1385 (Springer-Verlag, Berlin, 1987).

[41] I. Müller and T. Ruggeri, *Extended Thermodynamics*, Springer Tracts in Natural Philosophy, Vol. 37 (Springer-Verlag, New York, 1993).

[42] R. P. Drake, P. Keiter, C. Kuranz, G. Malamud, M. Manuel, C. Di Stefano, E. Gamboa, C. Krauland, M. MacDonald, W. Wan, R. Young, D. Montgomery, C. Stoeckl, and D. Froula, Study of shock waves and related phenomena motivated by astrophysics, J. Phys.: Conf. Ser. **688**, 012016 (2016).

[43] M. Hatifi, G. Di Molfetta, F. Debbasch, and M. Brachet, Quantum walk hydrodynamics, Sci. Rep. **9**, 2989 (2019).

[44] C. H. Alderete, S. Singh, N. H. Nguyen, D. Zhu, R. Balu, C. Monroe, C. Chandrashekar, and N. M. Linke, Quantum walks and Dirac cellular automata on a programmable trapped-ion quantum computer, Nat. Commun. **11**, 1 (2020).

[45] M. Saeedi and M. Pedram, Linear-depth quantum circuits for n-qubit Toffoli gates with no ancilla, Phys. Rev. A **87**, 062318 (2013).

[46] A. Carrera Vazquez and S. Woerner, Efficient State Preparation for Quantum Amplitude Estimation, Phys. Rev. Appl. **15**, 034027 (2021).

[47] A. N. Soklakov and R. Schack, Efficient state preparation for a register of quantum bits, Phys. Rev. A **73**, 012307 (2006).

[48] A. G. Rattew and B. Koczor, Preparing arbitrary continuous functions in quantum registers with logarithmic complexity, arXiv:2205.00519 (2022).

[49] H.-Y. Huang, R. Kueng, and J. Preskill, Predicting many properties of a quantum system from very few measurements, Nat. Phys. **16**, 1050 (2020).

[50] I. Hamamura and T. Imamichi, Efficient evaluation of quantum observables using entangled measurements, npj Quantum Inf. **6**, 56 (2020).

[51] R. Somma, G. Ortiz, E. Knill, and J. Gubernatis, Quantum simulations of physics problems, Int. J. Quantum. Inform. **01**, 189 (2003).

[52] F. Acasiete, F. P. Agostini, J. K. Moqadam, and R. Portugal, Implementation of quantum walks on IBM quantum computers, Quant. Info. Proc. **19**, 426 (2020).

[53] C. Huerta Alderete, S. Singh, N. H. Nguyen, D. Zhu, R. Balu, C. Monroe, C. Chandrashekar, and N. M. Linke, Quantum walks and Dirac cellular automata on a programmable trapped-ion quantum computer, Nat. Commun. **11**, 3720 (2020).

[54] P. Coles and K. Spencer, A wave-mechanical approach to cosmic structure formation, Mon. Not. R. Astron. Soc. **342**, 176 (2003).

[55] P. Sikivie and Q. Yang, Bose-Einstein Condensation of Dark Matter Axions, Phys. Rev. Lett. **103**, 111301 (2009).

[56] R. E. Wyatt, *Quantum Dynamics with Trajectories*, Interdisciplinary Applied Mathematics (Springer Science & Business Media, New York, 2005).

[57] M. Tsubota, M. Kobayashi, and H. Takeuchi, Quantum hydrodynamics, Phys. Rep. **522**, 191 (2013).

[58] G. Manfredi, How to model quantum plasmas, Fields Inst. Commun. **46**, 263 (2005).

[59] F. Haas, *Quantum Plasmas: An Hydrodynamic Approach*, Vol. 65 (Springer Science & Business Media, NY, United States, 2011).

[60] M. Bonitz, Z. A. Moldabekov, and T. S. Ramazanov, Quantum hydrodynamics for plasmas-quo vadis? Phys. Plasmas **26**, 090601 (2019).

[61] P. Arnault, G. Di Molfetta, M. Brachet, and F. Debbasch, Quantum walks and non-Abelian discrete gauge theory, Phys. Rev. A **94**, 012335 (2016).

[62] P. Arnault and F. Debbasch, Quantum walks and discrete gauge theories, Phys. Rev. A **93**, 052301 (2016).

[63] G. Di Molfetta, M. Brachet, and F. Debbasch, Quantum walks as massless Dirac fermions in curved space-time, Phys. Rev. A **88**, 042301 (2013).

[64] P. Arnault and F. Debbasch, Quantum walks and gravitational waves, Ann. Phys. **383**, 645 (2017).

[65] F. Debbasch, Discrete geometry from quantum walks, Condens. Matter **4**, 40 (2019).

[66] G. Di Molfetta, F. Debbasch, and M. Brachet, Nonlinear optical Galton board: Thermalization and continuous limit, Phys. Rev. E **92**, 042923 (2015).

[67] M. Lubasch, J. Joo, P. Moinier, M. Kiffner, and D. Jaksch, Variational quantum algorithms for nonlinear problems, Phys. Rev. A **101**, 010301(R) (2020).

[68] P. S. Correia, P. C. Obando, R. O. Vallejos, and F. de Melo, Macro-to-micro quantum mapping and the emergence of nonlinearity, Phys. Rev. A **103**, 052210 (2021).

[69] T. M. Wintermantel, Y. Wang, G. Lochead, S. Shevate, G. K. Brennen, and S. Whitlock, Unitary and Nonunitary Quantum Cellular Automata with Rydberg Arrays, Phys. Rev. Lett. **124**, 070503 (2020).

[70] Y. M. Bunkov, Quantum magnonics, J. Exp. Theor. Phys. **131**, 18 (2020).

[71] M. Kjaergaard, M. E. Schwartz, J. Braumüller, P. Krantz, J. I.-J. Wang, S. Gustavsson, and W. D. Oliver, Superconducting qubits: Current state of play, Annu. Rev. Condens. Matter Phys. **11**, 369 (2020).